Results of the Development of a Tandem-bladed Centrifugal Compressor Stage

David Hlaváček[1,*], Daniel Hanus[2]

[1]Czech Technical University in Prague, Faculty of Mechanical Engineering, Department of Aerospace Engineering, Karlovo nám. 13, 121 35, Praha 2, Czech Republic
[2] Czech Technical University in Prague, Faculty of Transportation Sciences, Department of Air Transport, Horská 3, 128 03, Praha 2, Czech Republic

Abstract

This paper summarizes the results of the development of an advanced centrifugal compressor stage for aeronautical applications, using so-called tandem impeller blading. During the development, performed by means of numerical computations, a configuration was found which improved all the integral stage parameters investigated, i.e. its total pressure ratio, isentropic efficiency and flow capacity. These results were achieved by modifying the shape of the axial inducer vane, the circumferential position of the radial blades against the axial blades, and the radial blade transversal lean angle. At the same time, recommendations for future development of this type of stages were defined. It can be stated that a correctly designed tandem-bladed stage can achieve significantly higher values of the integral parameters compared to a conventional stage with the same outer dimensions and thus contribute to reducing aeronautical engine fuel consumption, dimensions and weight.

Keywords: centrifugal compressor; tandem blading; inducer; exducer; CFD; total pressure ratio; isentropic efficiency

1. Introduction

The term *tandem impeller blading* refers to centrifugal compressor impeller blades, divided transversely into two parts after the inducer (see Fig. 1). The inducer part of the blades is thus made up of an axial blade vane while the exducer part consists of standard radial blading, including splitter blades. The trailing edges of the inducer blades are placed inside every second exducer passage.

This arrangement positively affects the formation of boundary layers on the impeller blade surfaces. After the inducer parts of the blades, its growth is interrupted, and the resulting wake flow is directed into the exducer channel. This should result in reducing the size of the wake region at the impeller exit which, in turn, leads to increasing the isentropic efficiency of the stage.

The first research report about tandem impeller blading by Boyce and Nishida appeared as early as 1977. Since then, however, papers concerning this topic have only been scarce. In [5] (published in 2002), the authors explicitly mention the near non-existence of guidelines for designing tandem impeller blading.

At the Department of Aerospace engineering, this topic was already examined in 2005, concluded by [2] in which the authors stated that tandem blading had a potential to improve the isentropic efficiency of a centrifugal compressor stage. Regrettably, no further research leading to an optimum geometry or the design guidelines was made.

Thus, the goal of the present research was to prove the assumptions regarding the positive influence of tandem blading on the compressor stage flow field (and, of course, its integral parameters), to find an optimum geometry which would ensure a greater isetropic efficiency while at least maintaining the same total pressure ratio and flow capacity, and also to define the guidelines or recommendations for designing this type of stages.

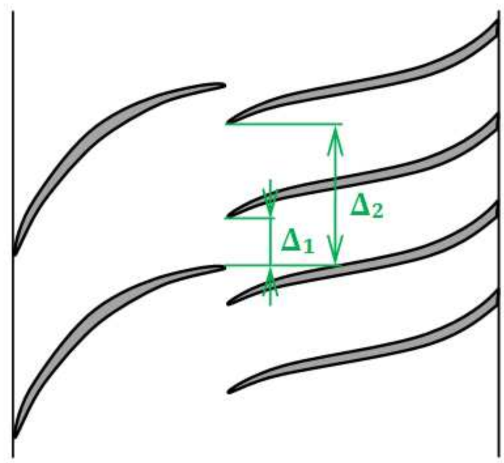

Fig. 1. *The tandem blading concept*

Our family of tandem-bladed stages was based on a conventional stage (further called the *Baseline Stage*), originally developed by Walter Engines, a.s. (now GE Aviation Czech) in cooperation with VZLÚ, a.s. (Aerospace Research and Test Establishment).

The research proceeded as follows: First, a numerical model of the baseline stage was developed and its results were compared to the experimental data. Then, after the model of the baseline stage was validated, further computations were made which already involved tandem blading.

During the blading optimization process, three main parameters were modified – the shape of the axial inducer vane, the relative circumferential position of the in-

*Contact the author at: David.Hlavacek@fs.cvut.cz

ducer and exducer, and the exducer blade transversal lean angle. The innovative impeller geometry maintained the shape of the impeller meridional section and the number of both main blades and splitter blades (or, in the tandem arrangement, axial and radial blades) as well as the angles of the absolute velocities at impeller inlet and outlet (i.e. no prewhirl, the same backsweep angle). The diffuser also remained unchanged.

Since the outer dimensions are the same, a new tandem-bladed impeller can simply be mounted into the existing engine and help improve its parameters without using any other external devices. The same approach, of course, can also be applied to centrifugal compressor stages used by other engines.

The results of the computations showed the potential of tandem blading to significantly improve the integral parameters of the stage compared to the baseline stage.

2. The Baseline Stage

Before the tandem-bladed stage could be developed and its advantages proved, a numerical model of the baseline stage had to be configured. The baseline stage was chosen from a family of experimental compressor stages which comes from the M602 turboprop engine and is known by number 410. This family of stages was developed by Walter Engines, a.s. (now GE Aviation Czech) in cooperation with VZLÚ, a.s. (Aerospace Research and Test Establishment). The geometries and performance curves of all these stages were available which made it possible to select the stage (410.B1) which was the most suitable for this type of modification.

2.1. Numerical model configuration

The computational model of the baseline stage was made using the ANSYS software package. First, the geometry of the stage was carried over from [6] using BladeGen and DesignModeler. Afterwards, the computational mesh was generated using TurboGrid (impeller mesh) and Meshing (diffuser mesh), the boundary conditions and other model properties were set in CFX-Pre, the preprocessing utility, and finally, the governing equations were solved using the CFX solver and its results compared to the experiment.

The computational mesh of each impeller channel consisted of 400,000 hexahedral cells in a structured O/C/H-grid and the diffuser mesh of 97,000 tetrahedral cells, accompanied by hexahedral cells near the walls to model the boundary layers. For the purpose of saving computational time during the calibration process which involves a lot of computational runs, one impeller channel together with one diffuser channel was modeled.

The governing equations were discretized by the second order upwind scheme. As a convergence criterion, the root mean squares of the residuals were used.

The total pressure at the impeller inlet and mass flow at the diffuser outlet were chosen as boundary conditions for the baseline stage model. The flow inside the stage was assumed to be steady (which, according to [3], can be a reasonable approximation, widely used in practice).

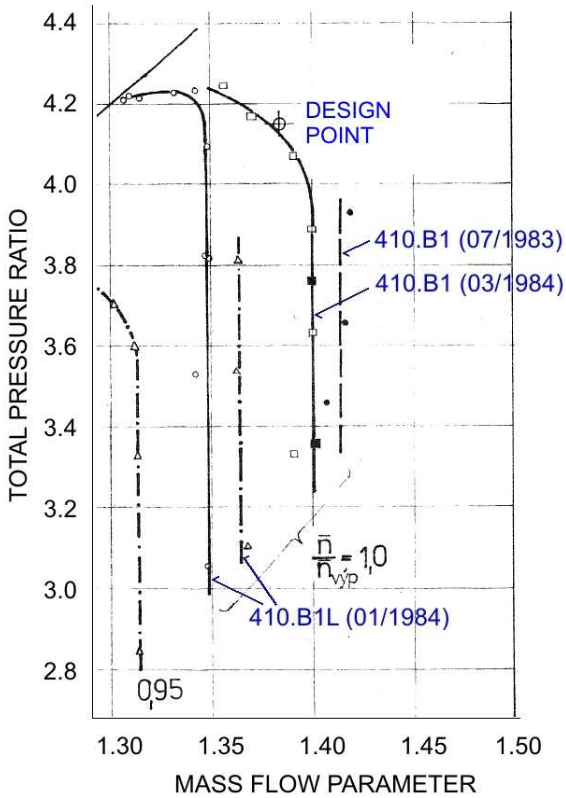

Fig. 2. *The baseline stage measured performance curve at design speed*

The interface between the impeller and the diffuser was modeled using the mixing plane model

For describing the properties of air, a semi-ideal gas model was used in which the constant pressure specific heat capacity c_p and the dynamic viscosity μ depend on temperature.

For modeling turbulence, the RNG k-ε model was chosen which provides a reasonable accuracy without investing an excessive amount of computational time This model was recommended by the authors of [1] for modeling flow fields inside small-scale radial tubromachinery. During the validation process, other models were also tested and the RNG k-ε model proved to be the most accurate. For modeling flow near the walls, this model was accompanied by a scalable wall function.

2.2. Numerical model results

After some diffuser mesh refinement, the numerical model described the performance curve at 100% design speed with a satisfying accuracy.

The measured performance curve (Fig. 2) was estimated very closely in terms of total pressure ratio (Fig. 4). The mass flow parameter at choke limit was overestimated by 1.6% in comparison with the measurement made in March 1984. However, as Fig. 2 shows, the measured choke limit was 1% higher when measured in July 1983. The isentropic efficiency was in all cases overestimated by a nearly constant value o 1.5%.

At lower speeds (90% and 80% design speed), the model accuracy was also sufficient. The maximum total pressure ratio error was about 5% while the isentropic efficiency error did not exceed 2.5%.

With these results in mind, the computational model of the baseline stage could be considered validated. Thus, the examination of various arrangements of tandem-bladed stages could be based on it. The numerical values, of course, will always be rather inaccurate. However, the model is accurate enough for comparative purposes and for proving whether the tandem impeller blading has a potential for improving the integral parameters of the stage.

When the suitability of the baseline stage numerical model was proved, the properties of the flow field inside the impeller were also examined. Apart from other things (relative Mach number distribution at 50% span, eddy viscosity distribution at 75% span), the appearance of the relative velocity radial component distribution at the impeller exit was observed. This is an important measure of the intensity of secondary flow. In an ideal case, the patterns should be the same in the two different sets of exducer channels (i.e. between the main blade suction side and the splitter blade pressure side, and between the main blade pressure side and the splitter blade suction side, respectively) As stated in [7], this helps reduce mixing losses inside the diffuser. The low-momentum fluid zone (or *wake zone*) at the impeller exit should be as small as possible. These are also the goals of the tandem-bladed stage development.

From the actual distribution of radial relative velocity at the impeller outlet (Fig. 3), it can be observed that the

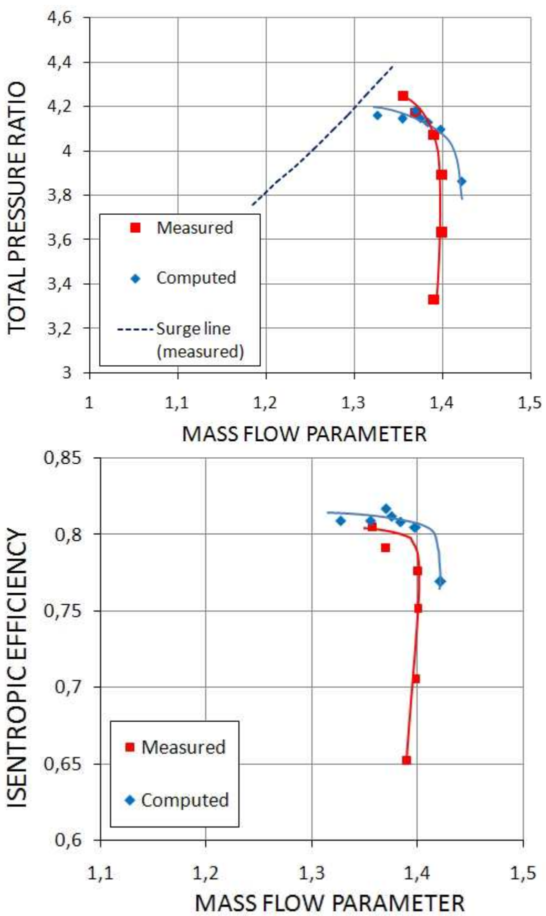

Fig. 4. *The performance curve and isentropic efficiency curve of the baseline stage at 100% speed*

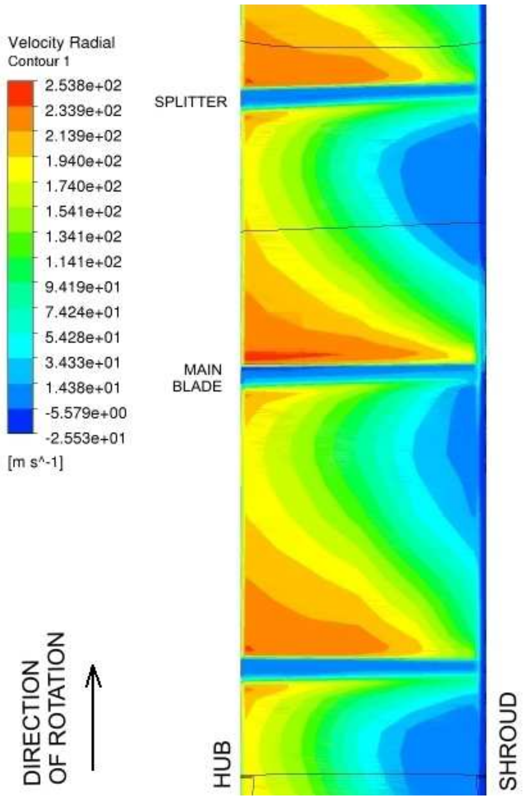

Fig. 3. *Radial relative velocity distribution at the baseline stage impeller outlet*

velocity fields in the two sets of channels visibly differ from each other.

To quantify the properties of the velocity fields at the impeller channel outlets, the sizes of wake regions were calculated in each channel. Let the wake region be defined as a region with a radial velocity less or equal to 20% of the maximum velocity in the pair of channels observed. The size of this region will be given in % of the channel area. For the baseline stage, the following sizes of the wake regions were computed:

Table 1: *Sizes of wake regions at the impeller outlet of the baseline stage*

Channel	**Size (% channel area)**
Rear main blade S.S. – Splitter P.S.	26.41
Rear main blade P.S. – Splitter S.S.	17.26

From these values, it is apparent that there is still some space for improving the evenness of the velocity patterns between the two sets of channels. The tandem-bladed arrangement is assumed to improve these parameters.

3. Stages Created by Interrupting the Existing Blading

After the validation had been finished, the search for an optimum arrangement of the tandem impeller blading started. In its beginning, the effort primarily focused on finding the most suitable axial inducer vane which would have the potential for considerably improving the parameters of the stage. Afterwards, modifications to the exducer blading would be made so that the two vanes could cooperate with each other successfully.

3.1. Stage 0

Before any new blade shape was designed for the axial inducer vane (AIV), a trial was made to interrupt the existing blading and to test its performance at two circumferential positions of the radial blades against the axial blades: 50/50%, and 92/8% of the axial vane pitch . These stages were named Stage 01 and 02, respectively. This was done in order to examine whether the interruption of the boundary layer growth alone (and, of course, the resulting wake flow directed into the middle of the downstream channel) can improve the flow field and the compressor parameters, or there is a need to do other modifications to the blading. The computation was made at the baseline stage design speed (n = 25,000 rpm).

Neither of these two configurations proved to be successful. The Stage 01 impeller with the position of radial blades at 50/50% pitch achieved a total pressure ratio near the design point of 3.872 which is about 0.27 units and 6.5% less compared to the baseline stage. The maximum mass flow parameter was 1.27. This is 0.13 units and 9.3% less than the baseline stage had.

In the Stage 02 impeller, the radial blades had a position of 92/8% pitch. In this configuration, the blades were, practically, just interrupted and the wake flow downstream of the axial inducer vane was not directed into the middle of the exducer channel but, on the contrary, the leading edges of one half of the radial blades were virtually exposed to this wake flow. Stage 02 achieved the same total pressure ratio near the design point of 3.872. The maximum mass flow parameter – which was 1.34 – was somewhat higher compared to the above-mentioned stage but it still does not achieve the parameters of the baseline (0.06 units and 4.2% less). This brings us to a conclusion that, for this impeller arrangement, changing the circumferential position of

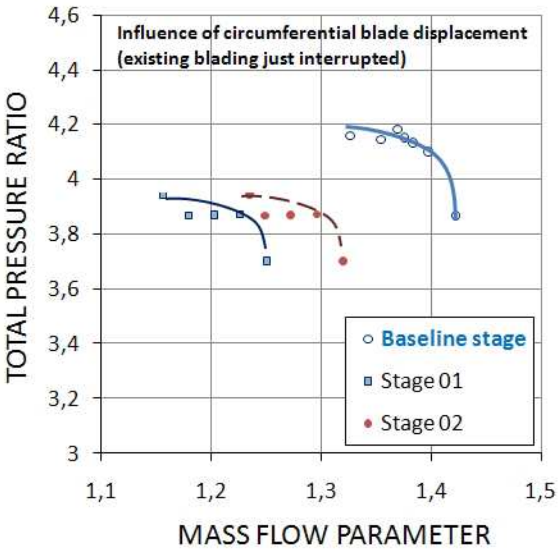

Fig. 6. *Performance curves of stages 01 and 02*

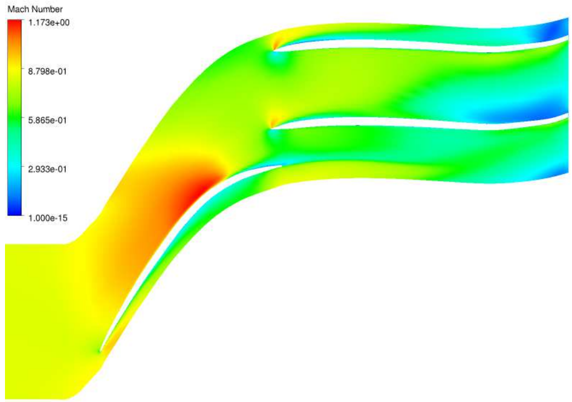

Fig. 5. *Relative Mach number distribution at 50% span inside the Stage 01 impeller at Q = 1.227 , π = 3.872*

the exducer blades against the inducer blades shifts the performance curve in the horizontal direction (see Fig. 7).

After these computations, a conclusion was made that the front parts of former centrifugal compressor main blades could not be used successfully as a part of tandem blading. Therefore, the axial inducer vane had to be designed anew.

4. Stages with Newly Designed Axial Inducer Vanes

4.1. Stage A

The next step was using an inducer vane originally designed for axial compressors. This vane was designed using a method published in a textbook by S. Farokhi [3]. The blades had circular-arc centerlines and their outer contours also consisted of circular arcs, except the elliptical leading and trailing edges. The design was made at the inner, mean, and outer impeller diameters.

First, the total pressure ratio of 1.1 was selected for such vane. Other design constraints included the design axial absolute velocity at the baseline stage inlet which was 150 m.s^{-1}, the design shaft speed of 25,000 rpm, the design point angle of attack of 4 deg, and the original inlet total pressure and temperature ($p_{1,tot}$ = 94,892 Pa,

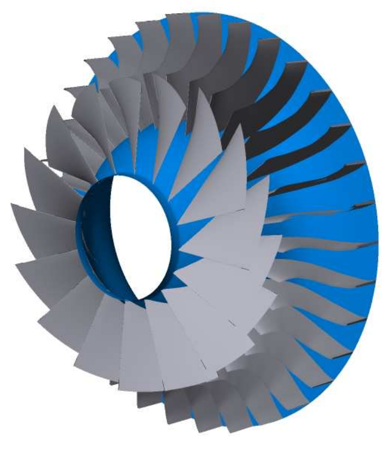

Fig. 7. *The Stage A impeller*

$T_{1,tot}$ = 303 K).

This newly designed vane was, at first, incorporated into an impeller with the original splitter blades. This stage was named Stage A0. As can be seen in Fig. 9, Stage A0 suffered from large incidence losses at the radial blade leading edges and its parameters were even worse than Stages 01 and 02 had (near-design-point total pressure ratio 3.730, maximum mass flow parameter 1.20). Therefore, a decision was made to modify the front parts of the radial blades, i.e. to change their camberlines from the leading edges up to one-third of their lengths.

So, afterwards, the front parts of the radial blades were modified in such a way that the stagger angle at their leading edges corresponded to the stagger angle at the axial inducer vane trailing edges. The first stage with this impeller was named Stage A1. Its radial blades were placed in 32/82 % pitch at the hub. This initial choice corresponded to selecting 50/50 % pitch in the ANSYS BladeGen software. The total pressure ratio of this stage

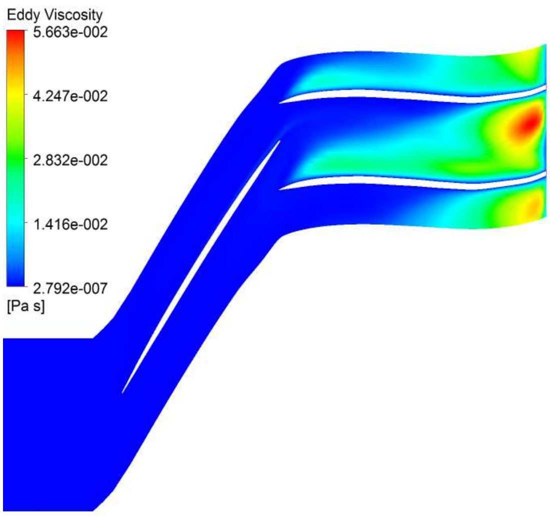

Fig. 8. *Eddy viscosity distribution at 75% span inside the Stage A0 impeller at Q = 1.188 , π= 3.563*

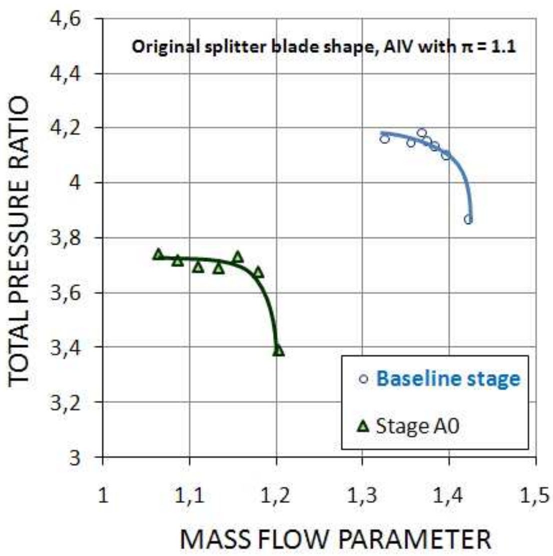

Fig. 10. *Stage A0 performance curve at 100% design speed*

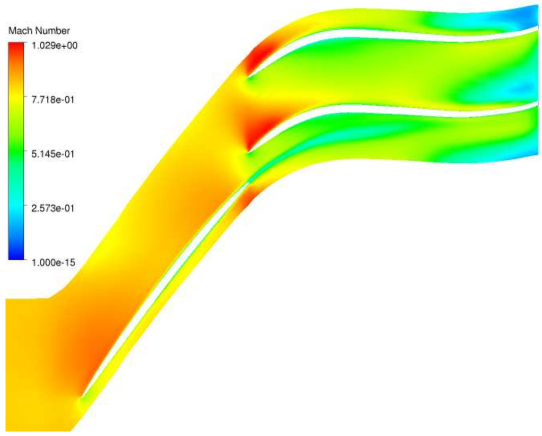

Fig. 9. *Relative Mach number distribution at 50% span inside the Stage A3 impeller*

was then about equal to that of the baseline stage (although it had a rather oscillating manner).

The mass flow parameter was slightly lower (by 0.057 units/4% at the choke limit) and the isentropic efficiency was about 2% lower compared to the baseline stage. The computations were, as in the previous cases, performed at the baseline stage design speed.

Afterwards, when the circumferential position of the radial blades was slightly modified, the potential of tandem blading was finally revealed.

While Stage A2 (37/87% pitch at the hub) performed only slightly better than Stage A1, Stage A3 (39/89% pitch at the hub) showed the best parameters in this group of stages, exceeding the total pressure ratio of the baseline stage by 0.15 units (3.6%) while, in the best case, achieving the same isentropic efficiency. In this impeller, the axial blades were nearest to the suction sides of the radial blades.

Thus, by this computational investigation, it was also found out that tandem-bladed impellers can, in certain cases, be quite sensitive to the radial blade position. This gives some space to maneuver to the future designers of this type of impellers.

From the distribution of radial relative velocities at the impeller outlet (Fig. 12), it can be seen that the velocity patterns in the two sets of exducer channels are very similar to each other. The sizes of wake zones only differ by 0.7%. However, both of them are still quite large – about one-quarter of each channel is occupied by the low-momentum fluid. This, along with the still insufficient integral parameters of the stage, made it necessary to further optimize the tandem-bladed stage.

Table 2: *Sizes of wake regions at the Stage A3 impeller outlet*

Channel	**Size (% channel area)**
Rear main blade S.S. – Splitter P.S.	25.23
Rear main blade P.S. – Splitter S.S.	24.53

Nevertheless, Stage A set the route to follow during the further optimization: to design another axial inducer vane according to the rules used for axial compressors, then make it properly cooperate with the radial blading

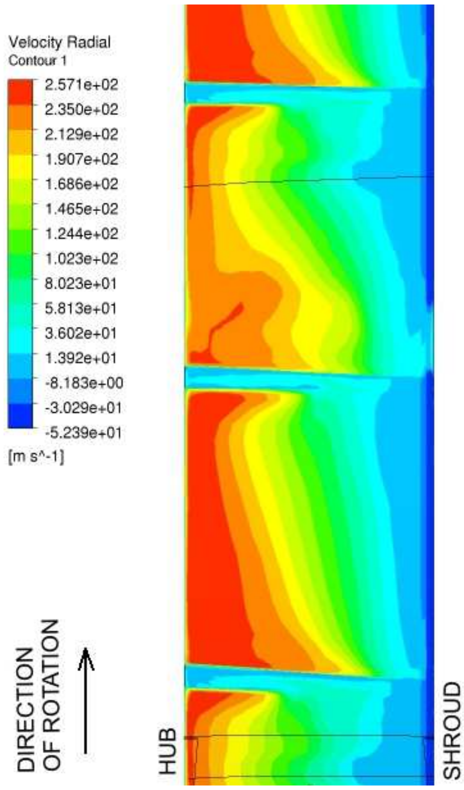

Fig. 14. *Radial relative velocity distribution at the Stage A3 impeller outlet*

by modifying the front parts of the radial blades and, finally, to find an optimum position of these against the axial blades.

4.2. Stage B

Since the axial vane used in Stage A was a rather conservative choice (as it was also confirmed by the results of the computation), the next step was designing a stage containing an axial vane with a total pressure ratio of 1.2. The other AIV design constraints remained the

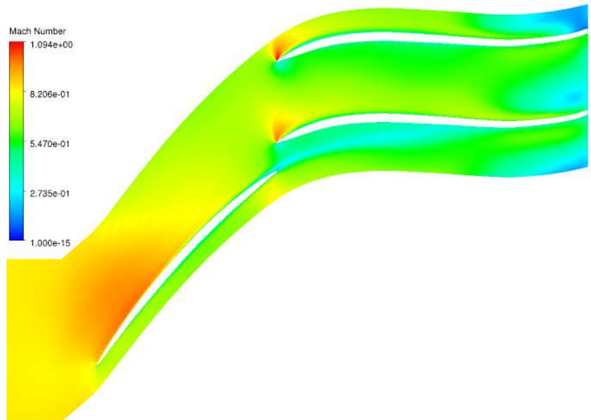

Fig. 12. *Relative Mach number distribution at 50% span inside the Stage B1 impeller at Q = 1.365, π= 4.379*

same, including the angle of attack of 4 deg.

The radial blades were also modified. Just as in the previous case, the stagger angles of the radial blade leading edges were changed to be the same as the axial vane trailing edge stagger angles, and the radial blades were modified up to one-third of their camberlines. Again, three positions of the radial blades against the axial inducer vane were tested (stages B1 to B3). This time, the parameters achieved by the respective stages were not so sensitive to the circumferential position of the radial blades. However, the performance curves in one case out of the three (Stage B2) had an oscillating manner. This was the one with the radial blade leading edges nearest to the axial blade trailing edges (Δ_1 = 18% pitch at the hub). This effect is the same as in the case of stages A1 to A3. Stage A1 (Δ_1 = 32%, Δ_2 = 82% pitch at the hub) also had considerable oscillations of total pressure ratio along its performance curve. From these results, we can conclude that if the circumferential gap between the radial blade leading edges and the axial blade trailing edges is too small, the stage will suffer from oscillations of the total pressure ratio as the mass flow changes.

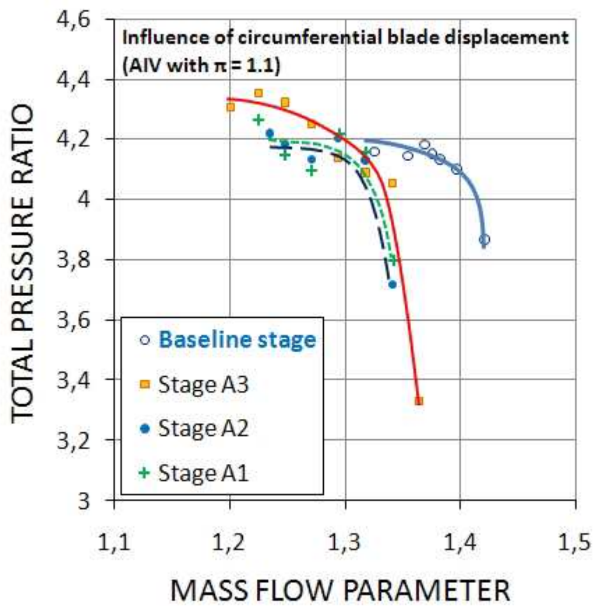

Fig. 11. *Stage A performance curves at 100% design speed*

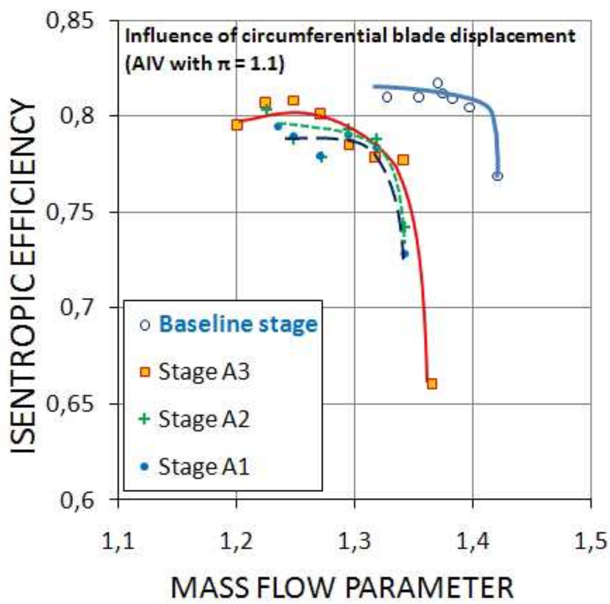

Fig. 13. *Stage A isentropic efficiency curves at 100% design speed*

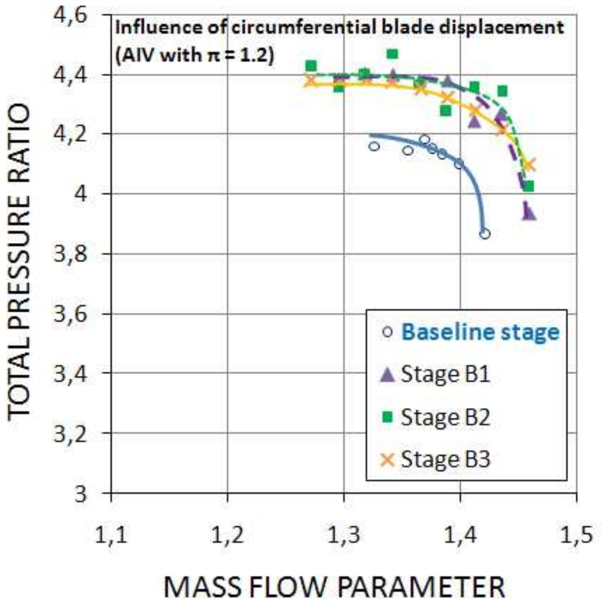

Fig. 16. *Stage B performance curves at 100% design speed*

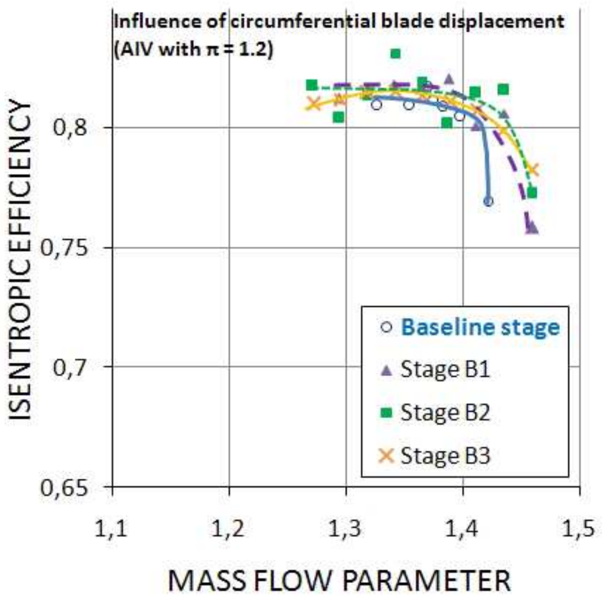

Fig. 17. *Stage B isentropic efficiency curves at 100% design speed*

From this series of stages, Stage B1 performed the best, having a greater total pressure ratio (by about 0.2 units which is 5%) and also a greater isentropic efficiency (by about 1%). The mass flow parameter at choke limit was increased by 2.6%. Moreover, the values of the total pressure ratio and isentropic efficiencies were also stable, without any significant oscillations. The radial blades of Stage B1 had a position of 20/70% pitch at the hub. This initial choice was determined by the middle of the range of positions that the ANSYS BladeGen software allowed for. Stage B2 then had a position of 18/68% pitch while Stage B3 had 22/72% pitch.

These computations confirmed the ability of tandem impeller blading to significantly improve the parameters of a centrifugal compressor stage. Obviously, this statement is only based on a qualitative comparison (which was, in fact, the main purpose we used the CFD computations for). The exact values of total pressure ratios and isentropic efficiencies must be determined by measurement.

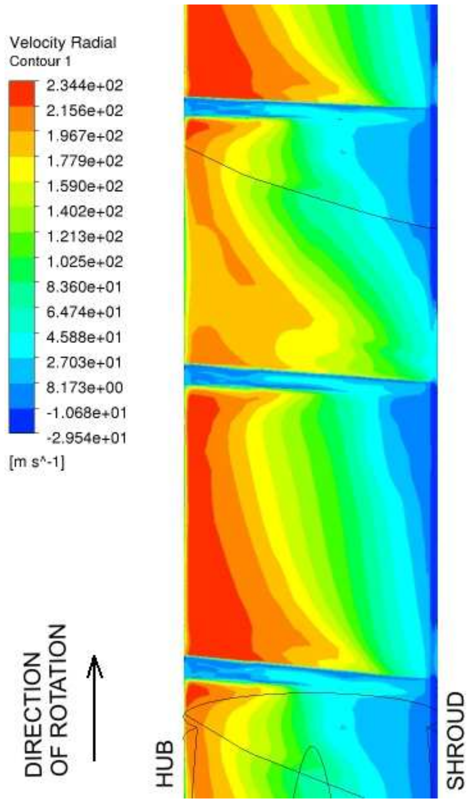

Fig. 15. *Radial relative velocity distribution at the Stage B1 impeller outlet*

It also became clear that the tandem impeller blading affects the stage total pressure ratio to a greater extent than it does with its isentropic efficiency and mass flow parameter.

As for the radial velocity field at the impeller outlet (Fig. 16), the relative sizes of both wake regions have now reduced themselves in comparison with the baseline stage and they are also closer to each other (a difference of 3.13% instead of 9.15%). Nevertheless, the values achieved by Stage A are still the closest to each other.

Especially the channel between the rear part of the former main blade S.S. and the former splitter P.S. achieved a significant reduction of the wake region size (by as much as 7.13%). This confirms the positive contribution of the tandem blading to the quality of the flow field leaving the impeller.

Table 3. *Sizes of wake regions at the Stage B1 impeller outlet*

Channel	Size (% channel area)
Rear main blade S.S. – Splitter P.S.	19.28
Rear main blade P.S. – Splitter S.S.	16.15

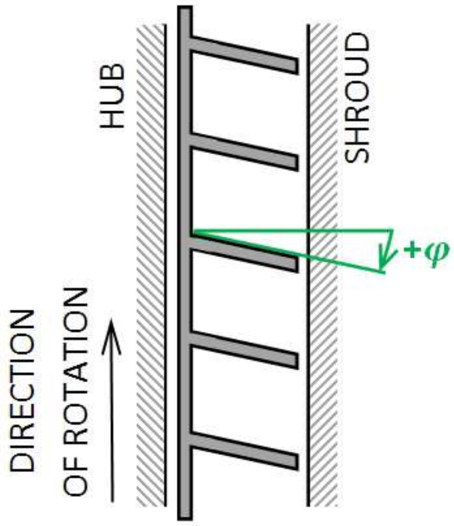

Fig. 18. *The explanation of the lean angle at the impeller outlet*

5. Stages with Transversal Blade Lean

Another modification to the tandem blading to be made was a transverse lean of the radial blades at the impeller outlet.

As stated in [7], leaning the blades introduces a force component in the hub-to-shroud direction into the flow field. When done the right way (so that the hub 'precedes' the shroud – see Fig. 18), it reduces the blade loading near the hub while increasing it near the shroud. Thus the blade loading is reduced, particularly in the rear part of the impeller. This should lead to weakening the hub-to-shroud secondary flow in the meridional plane along the suction sides of the blades.

Three different lean angles (φ = 5°, 10°, 15°) at one radial blade circumferential position (38/88 % pitch at the hub) were tested and the respective stages were named F1.1 to F3.1. Then, for the lean angle of 10°

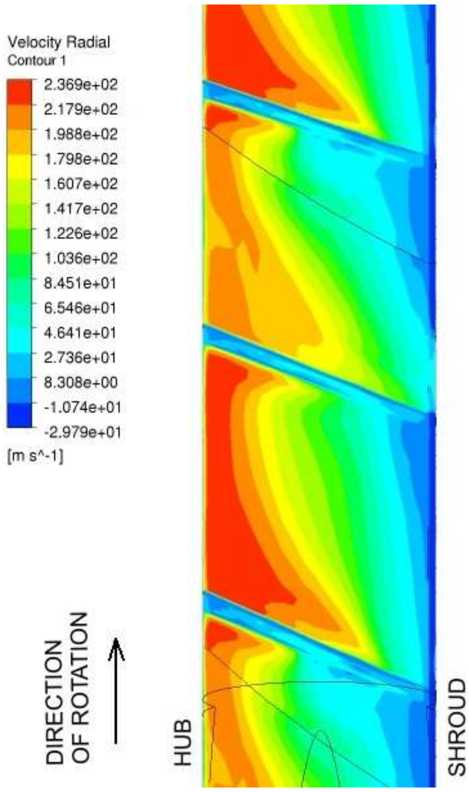

Fig. 20: *Radial relative velocity distribution at the Stage F2.3 impeller outlet*

(Stage F2.1) which had the best results, other two circumferential positions of the radial blades were tested (so that, apart from Stage F2.1, we obtained Stages F2.2 and F2.3). Stage F2.1 was chosen because of the oscillatory manner of the Stage F3.1 performance and efficiency curves, and of the lack of efficiency that the Stage F1.1 had.

Then, after testing the various circumferential positions of the radial blades, Stage F2.3 was chosen (33/83 % pitch at the hub) because of its greatest flow capacity and efficiency.

Leaning the radial blades had a positive effect on the

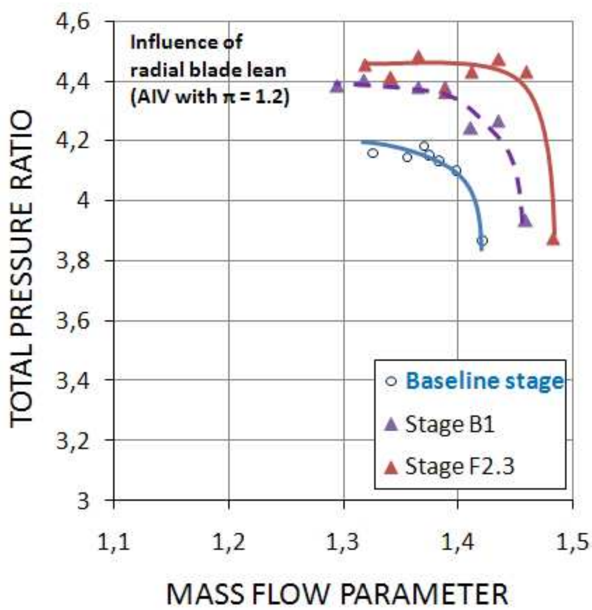

Fig. 19. *A comparison of the computed performance curves of the baseline stage, Stage B1, and Stage F2.3*

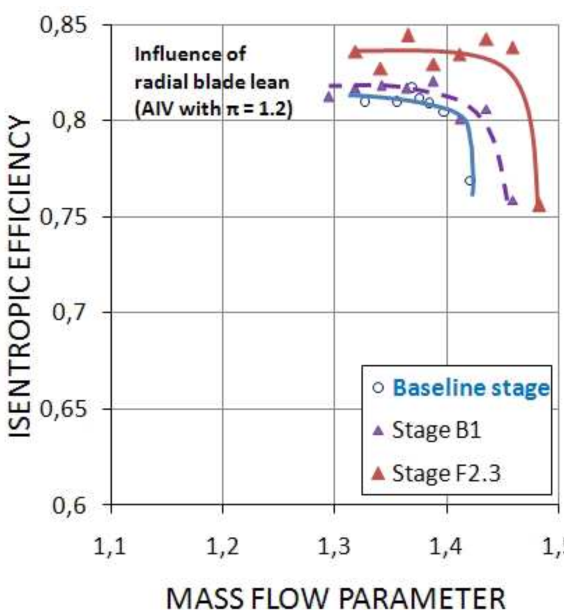

Fig. 21. *A comparison of the computed isentropic efficiency curves of the baseline stage, Stage B1, and Stage F2.3*

isentropic efficiency which increased by a further 1% compared to stage B1 (Stage F2.1), or by 2%, respectively (Stage F2.3). The total pressure ratio of Stage F2.3 increased by 2.3% while the stable mass flow range increased to the right side of the performance curve by about 1.6% (both results are compared to Stage B1). Stage F2.1 achieved only a slightly better total pressure ratio and about the same maximum mass flow parameter. The results achieved by Stage F2.2 (34/84% pitch at the hub) lay between the above-mentioned values. Therefore, stage F2.3 was considered an optimum configuration.

Table 4. *Sizes of wake regions at the Stage F2.3 impeller outlet*

Channel	Size (% channel area)
Rear main blade S.S. – Splitter P.S.	20.89
Rear main blade P.S. – Splitter S.S.	17.05

In case of Stage F, changing the circumferential position of the radial blades against the axial blades had, again, a considerable effect on the performance curves, especially in terms of the maximum mass flow parameter.

From the radial velocity pattern at the stage F2.3 impeller, it can be seen that both the sizes of the wake zone and the evenness of their distribution are slightly worse that Stage B had. It can therefore be stated that, for tandem-bladed impellers, leaning the radial blades can improve the isentropic efficiency, the mass flow parameter and, secondarily, the total pressure ratio. However, this improvement of stage performance does not involve the velocity patterns.

6. Comparison with the Modified Baseline

In order to clearly show the benefits of the tandem blading, a modified baseline stage was computed using the same computational model settings. The splitter blades and the corresponding rear portions of the main blades of the modified impeller were leaned transversely by an angle of 10 deg along all the splitter length (see Fig. 23).

The computation showed that the impeller with the modified splitter blades achieved an isentropic efficiency about 2.0% higher than the baseline did. The total pressure ratio and the mass flow parameter, however, remained almost the same.

The tandem-bladed stages F2.1 and F2.3 with leaned blades therefore still had a 5.6% / 7.8% greater total

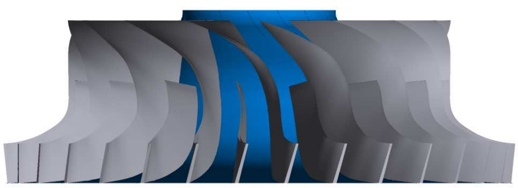

Fig. 23. *A model of the modified baseline stage impeller*

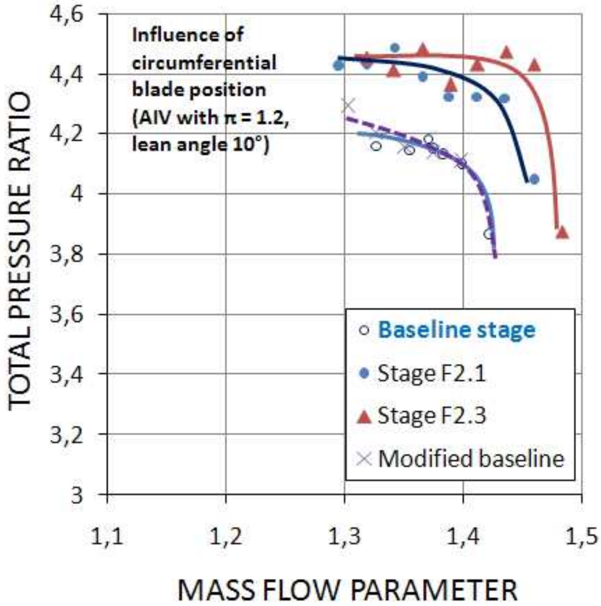

Fig. 24. *A comparison of the computed performance curves of the baseline stage, the modified baseline stage, Stage B1, Stage F2.1, and Stage F2.3*

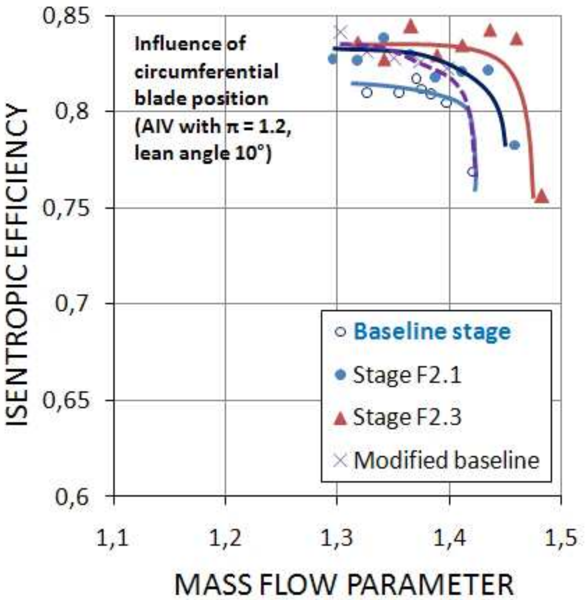

Fig. 22. *A comparison of the computed isentropic efficiency curves of the baseline stage, the modified baseline stage, Stage B1, and Stage F2.3*

pressure ratio and a 2.6% / 4.3% greater mass flow parameter in comparison with the modified baseline. However, the isentropic efficiencies of Stage F2.1 and the modified baseline are almost the same while Stage F2.3 achieves an about 1% greater efficiency.

From the computations involving Stage F and the modified baseline, it is clear that the tandem blading primarily affects the total pressure ratio of the stage. It also contributes to improving the stage isentropic efficiency but the relative increase (in %) is not as high. The stable mass flow range increases to both sides when tandem blading is used, both leaned and perpendicular.

7. An Alternative Concept

For future work on developing tandem-bladed stages, an alternative concept can be proposed. The basic idea is redesigning the inlet parts of every second radial blade in order to get equal portions of the total mass flow (i.e. 50/50 %) in each exducer channel. Thus, the radial blades which are placed downstream of the axial inducer vane will now consist of two different sets, one half of them having a different leading edge stagger angle than the other. The blade pitch at the impeller outlet should remain the same as it was before (i.e. equal for both sets of channels).

Note that when the tandem blading concept with the same radial blades was tested for the mass flow ratio between the two sets of channels, the result was, for example, 53.4/46.6 per cent in Stage A1 design point, i.e. a 6.8% difference between the two sets of exducer channels.

It is expected that the arrangement with equal mass flows will lead to a more even distribution of velocity patterns between the two sets of channels at the impeller exit. As already mentioned in Chap. 2.2, this evenness helps reduce mixing losses inside the diffuser. Moreover, since the total pressure losses are proportional to the second power of mass flow, the losses inside the impeller channels should be also more evenly distributed. And, finally, the sum of losses may even be reduced due to the fact that there will be no channel with a greater mass flow in which, as of now, an unneeded portion of kinetic energy is developed, only to be lost again by mixing.

The initial guess of the exducer channel inlet widths will be based on examining the velocity profile in the axial inducer vane outlet plane. Spanwise-averaged values of relative velocities will be plotted against the pitch coordinate and in the place in which the integral (i.e. the mass flow) reaches half its value, the leading edges of the modified radial blades will be placed.

Another thing which can be investigated during the future research is the influence of an eventual meridional gap between the inducer and exducer blades. During this stage of the research, this was not examined because of the limitations of the BladeGen software.

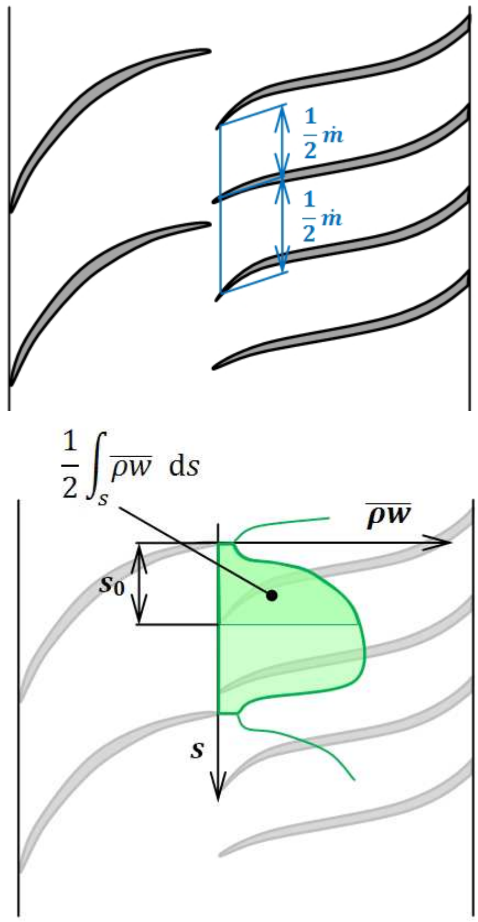

Fig. 25. *The alternative concept of tandem blading with equal mass flows in each channel between the splitter blades.*

8. Design Recommendations

Basic guidelines and recommendations for developing optimized tandem-bladed impellers, as found out during the research, can be summarized as follows:

1. The front parts of centrifugal compressor main blades are not suitable for being used as the axial inducer vane. Axial compressor blading should be used instead.

2. Tandem-bladed stages can be very sensitive to the circumferential position of the radial blades against the axial inducer vane. It is also not true that the best performance is achieved when the axial inducer vane trailing edges are placed halfway across the exducer channel. It is advisable that the suction sides of the axial blades be placed somewhat closer to the pressure sides of the adjacent radial blades. Placing them too close, however, will cause oscillations of the total pressure ratio along the performance curve.

3. The inlet stagger angles of the radial blades have an even greater influence than their circumferential position.

4. From pts. 1. and 3., it follows that when tandem blading is applied to an existing baseline impeller, it is recommended that both the inducer and exducer blading be redesigned (in order to cooperate with each other properly). Redesigning just one of the vanes does not bring the desired effect, as well as redesigning neither of them.

5. In comparison with a conventional stage with the same outer dimensions and number of blades, a properly designed tandem-bladed stage can achieve greater values of all the integral parameters examined in this thesis – the total pressure ratio, the isentropic efficiency, and the mass flow parameter. However, the relative increase of each parameter is different. It can be stated that tandem impeller blading primarily affects the total pressure ratio and the mass flow parameter and secondarily, the isentropic efficiency.

6. Tandem impeller blading can also reduce the sizes of wake zones at the outlet of the impeller exducer channels and make them more even when comparing the two sets of channels.

7. The properties of tandem-bladed stages, especially their isentropic efficiency, can be further improved

by leaning the radial blades transversely, as it is done with conventional stages .

8. The effects of tandem blading are more evident at high shaft speeds, close to the design point. As the computations showed, these effects are not that pronounced at lower speeds.

9. Conclusions

In this paper, results of the research of the properties of a centrifugal compressor stage with tandem impeller blading were summarized. These properties were examined by means of numerical computation.

The conventional compressor stage on which the development was based (the baseline stage) was selected among several experimental stages, its numerical model was configured and validated against experimental data. Afterwards, using this model, various arrangements of tandem-bladed stages were examined. The goal of the research was to reveal the true potential of tandem impeller blading and to find an optimum geometry of such impeller which would achieve greater values of isentropic efficiency (in comparison with a conventional stage with identical outer dimensions) while at least keeping the same total pressure ratio and mass flow parameter. This goal was fulfilled by Stage B and Stage F2.3..

Several recommendations and guidelines for developing this type of stages were also defined and further steps for developing the presented tandem-bladed stage were proposed. First, an alternative concept with two different sets of exducer blades should be examined and the geometry which would assure the same mass flows flowing in the two sets of channels should be found. The effect of axial spacing between the axial and radial vane should also be investigated.

Then, of course, selected tandem-bladed stages should undergo experimental research in order to quantify the increases of the stage integral parameters in comparison with the conventional geometry.

It can be concluded that, if properly designed, centrifugal compressor stages with tandem-bladed impellers do have a potential to increase the efficiency of aeronautical engine cycles, to reduce their weight and thus, eventually, spare large amounts of jet fuel.

List of symbols

c_p constant pressure specific heat capacity ($\mathrm{J{\cdot}kg^{-1}{\cdot}K^{-1}}$)
k turbulent kinetic energy ($\mathrm{m^2.s^{-2}}$)
$\dot{m}$ mass flow ($\mathrm{kg.s^{-1}}$)
p pressure (Pa)
Q mass flow parameter ($\mathrm{kg.s^{-1}{\cdot}K^{1/2}{\cdot}Pa^{-1}}$) *
s blade pitch (mm)
T temperature (K)
w relative flow velocity ($\mathrm{m.s^{-1}}$)

$\Delta_{1,2}$ radial blade position rel. to axial vane pitch (%)
ε turbulent eddy dissipation ($\mathrm{m^2.s^{-3}}$)
μ dynamic viscosity (Pa·s)
π total pressure ratio (1)
ρ density ($\mathrm{kg.m^{-3}}$)
φ transversal blade lean angle (deg)

Subscripts:
1 stage inlet
tot total temperature /pressure

* *Note:* the mass flow parameter is defined by the following formula:

$$Q = \dot{m}\,\frac{\sqrt{T_{1,\mathrm{tot}}}}{p_{1,\mathrm{tot}}} \qquad (1)$$

References

[1] AGHAEI TOG, R. – TOUSI, A. M. – TOURANI, A. *Comparison of turbulence methods in CFD analysis of compressible flows in radial turbomachines*. In: Aircraft Engineering and Aerospace Technology. Vol. 80, Iss.6., 2008. pp. 657-665. ISSN 1748-8842

[2] HANUS, Daniel et al. *First stage of the centrifugal compressor design with tandem rotor blades*. In: Proceedings of ISABE 2005. München, 2005.

[3] FAROKHI, Saeed. *Aircraft Propulsion*. J. Wiley & Sons, 2009. ISBN 978-0-470-03906-9. 786 pp.

[4] LIU, Zheji – HILL, D.L. *Issues surrounding multiple frames of reference models for turbo compressor applications*. In: International Compressor Engineering Conference, 2000. Paper 1369.

[5] ROBERTS, Douglas A. – KACKER, Suresh C. *Numerical Investigation of Tandem-Impeller Designs for a Gas Turbine Compressor*. In: Proceedings of ASME Turbo Expo 2001: Power for Land, Sea, and Air. Vol. 1: Aircraft Engine; Marine; Turbomachinery; Microturbines and Small Turbomachinery. Paper No. 2001-GT-0324. 12 pp.

[6] VANĚK,Václav – MATOUŠEK, Oldřich – VRÁTNÝ, Jiří. *Situační zpráva k výzkumu a vývoji dvoustupňového dvouhřídelového odstředivého kompresoru (DDOK). I. etapa výzkumu a vývoje nízkotlakého stupně VZLÚ 410*. Praha: VZLÚ, 1984.

[7] ZANGENEH, M. – GOTO, A. – HARADA, H. *On the design criteria for suppression of secondary flows in centrifugal and mixed flow impellers*. In: Journal of Turbomachinery. Vol. 120, No.4, 1998. pp. 723-735

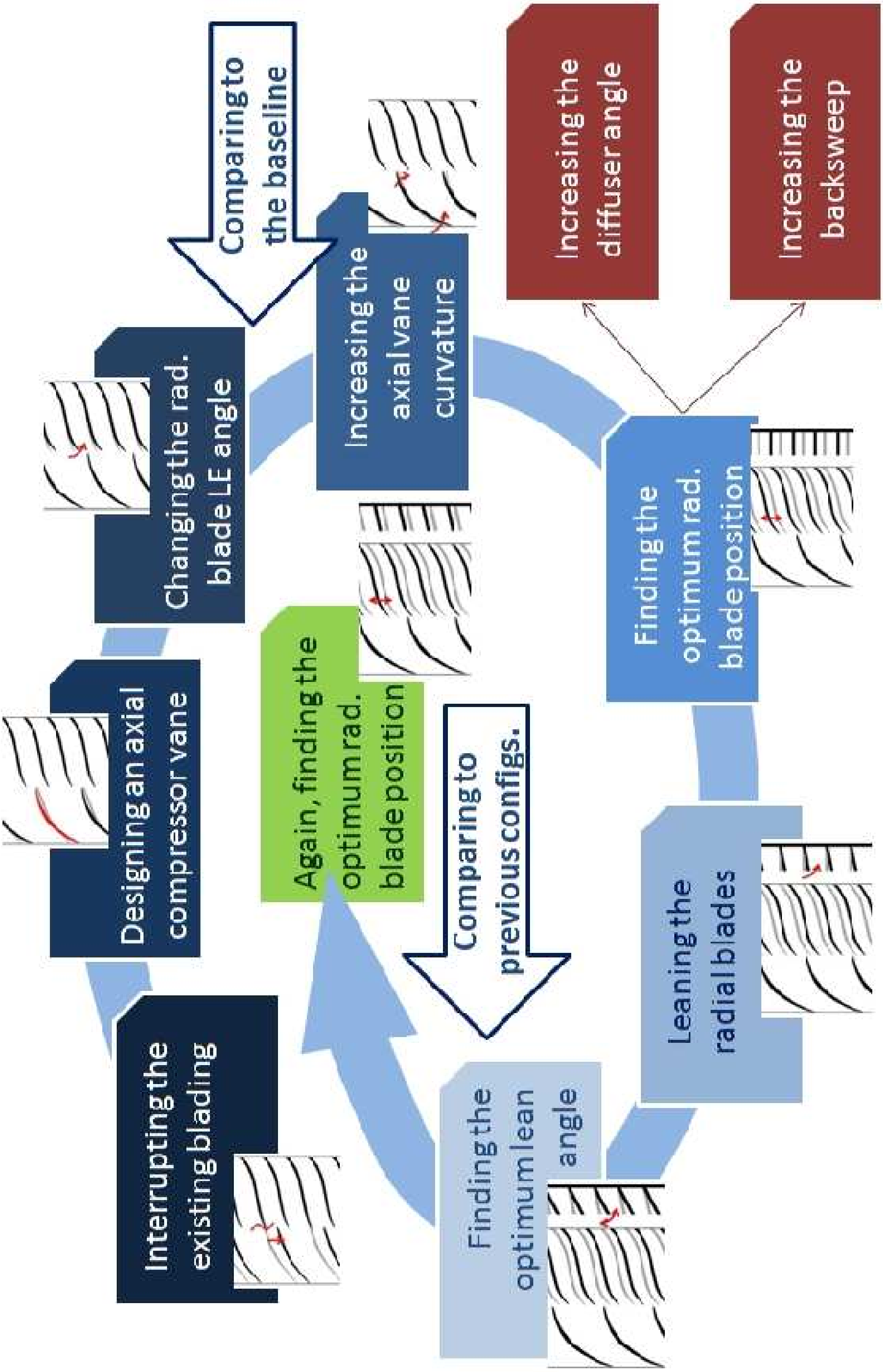

Fig. 26. *The tandem blading optimization road map. Ineffective modifications to the tandem blading (increasing the diffuser angle and the backsweep, not mentioned in this paper) are shown in dark red*